ESTIMATION OF ETHANOL CONTENT IN FLEX-FUEL VEHICLES USING AN EXHAUST GAS OXYGEN SENSOR: MODEL, TUNING AND SENSITIVITY

Kyung-ho Ahn, Anna G. Stefanopoulou*
Powertrain Control Laboratory
Department of Mechanical Engineering
The University of Michigan, Ann Arbor, USA

Mrdjan Jankovic
Ford Research and Advanced Engineering
Dearborn, Michigan 48121, USA

ABSTRACT

Throughout the history of the automobile there have been periods of intense interest in using ethanol as an alternative fuel to petroleum-based gasoline and diesel derivatives. Currently available flexible fuel vehicles (FFVs) can operate on a blend of gasoline and ethanol in any concentration of up to 85% ethanol. In all these FFVs, the engine management system relies on the estimation of the ethanol content in the fuel blend, which typically depends on the estimated changes in stoichiometry through an Exhaust Gas Oxygen (EGO) sensor. Since the output of the EGO sensor is used for the air-to-fuel ratio (AFR) regulation and the ethanol content estimation, several tuning and sensitivity problems arise. In this paper, we develop a simple phenomenological model of the AFR control process and a simple ethanol estimation law which can be representative of the currently practiced system in FFVs. Tuning difficulties and interactions of the two learning loops are then elucidated using classical control techniques. The sensitivity of the ethanol content estimation with respect to sensor and modeling errors is also demonstrated via simulations. The results point to an urgent need for model-based analysis and design of the AFR controller, the ethanol adaptation law and the fault detection issues in FFVs. Tuning and sensitivity issues are demonstrated via simulations and limitations are also discussed.

NOMENCLATURE

AFR_s Stoichiometric air-to-fuel ratio
$\widehat{AFR}_s$ Estimated stoichiometric air-to-fuel ratio
e Volume fraction of ethanol in gasoline-ethanol blend
$\widehat{e}$ Estimated volume fraction of ethanol in gasoline-ethanol blend
e_m Mass fraction of ethanol in gasoline-ethanol blend
MAF Mass air flow measured by a MAF sensor
T_m Manifold temperature measured by a manifold temperature sensor
W_{cyl} Air flow rate into the cylinder
$\widehat{W}_{cyl}$ Estimated air flow rate into the cylinder
W_f Fuel flow rate into the cylinder
W_{fb} Feedback fuel command
W_{ff} Feedforward fuel command
W_{ff1} Feedforward fuel command not compensated by the fuel puddle dynamics
X Aquino parameter denoting the wall-impacting portion of the injected fuel
α_{tr} Triggering signal for switching on ethanol adaptation
ε_{AFR_s} Estimation error in stoichiometric air-to-fuel ratio
θ Throttle angle
λ Ratio of actual AFR to stoichiometric AFR, λ is measured by an EGO sensor
ρ_{eth} Density of ethanol
ρ_{gsl} Density of gasoline
τ Aquino parameter denoting the vaporization time constant of the fuel puddle
τ_d Transport and induction-to-power delay from the cylinder input AFR to the exhaust AFR
τ_s Time constant of the exhaust oxygen sensor lag

INTRODUCTION

Petroleum-based fossil fuels are the dominant energy source for transportation. Recently, however, ethanol is being increasingly used as a fuel additive and is emerging as an alternative to carbon-neutral transportation. The advantage of ethanol, among others, is that it is a renewable fuel produced from biomass such

*Address all correspondence to annastef@umich.edu.

as barley, corn, wheat, sugar cane, trees and grasses. Therefore, to lessen dependence on fossil-based fuels, federal mandates, such as the Energy Policy Act of 2005 (EPACT 2005), require that 7.5 billion gallons of bio-fuel be produced in 2012. Ethanol can be blended with conventional gasolines in varying percentages. The blend is denoted by the EXX nomenclature, where XX represents the volumetric percentage of ethanol in the blend. The United States commonly uses E85 as an alternative to the normal E0 or gasoline fuel. In Brazil, however, the fuel blend also contains water and E100 refers to a blend of 93% ethanol and 7% of water [1]. Such fuel blends mixed with additional water are not considered in this paper. Vehicles that can operate on any blend of ethanol are called Flex Fuel Vehicles. These vehicles are designed to run on gasoline or a blend up to E85 in the U.S. and are currently being offered by many manufacturers.

The characteristics of ethanol differ from those of gasoline, as shown in Table. 1. Various effects of ethanol fuel on a spark ignition engine are well reported in [2]. Often ethanol fuel is associated with driveability and startability problems in cold and hot weather [3, 4] and at high altitude [5]. Existing FFVs achieve lower range (miles driven per tank) when operating on high ethanol content fuel due to its lower combustion heating value as compared to gasoline. However, as shown in Table. 1, ethanol has a higher octane ratio and therefore, a higher compression ratio and higher combustion efficiency can be obtained without knocking problems. Another advantage is that, the high vaporization heat can be used for charge cooling [6], thus improving further the knock resistance and potentially fuel economy. Given the effect of fuel variation, FFVs should embed engine calibration maps in their controllers and management systems to account for this variation. To accomplish this, the first task in a flex-fuel strategy is to estimate reliably the ethanol percentage. Although, this estimation is possible with the addition of a di-electric or electrochemical sensor in the fueling system, the reliability of these sensors has not yet been proven. Further, apart from the cost and reliability issues associated with such sensors, on-board diagnostic (OBD) requirements would require a redundant method for assessing the ethanol percent in order to diagnose the ethanol content sensor faults or degradation. Currently the ethanol content estimation depends on the AFR measurement through an exhaust gas oxygen (EGO) sensor immediately after refueling is detected. This trigger is used to avoid misclassifying ethanol content variations with actuator drifts or component aging. The ethanol detection period also needs to be as short as possible to reduce the probability of another (EGO or mass air flow (MAF) sensor, and/or injector) fault. Finally it is necessary to thoroughly understand and develop models for how uncertainty, sensor and actuator drifts propagate through the detection process and affect the ethanol content estimation. Basic discussion regarding the robustness of the estimation using the exhaust oxygen sensor feedback is provided in [7].

Table 1. PROPERTIES OF ETHANOL COMPARED WITH GASOLINE.

Property	Gasoline	Ethanol
Research Octane Number (RON)	92	111
Density (kg/m^3)	747	789
Heat of combustion (MJ/kg)	42.4	26.8
Stoichiometric air-to-fuel ratio	14.6	9.0
Boiling point (°C)	–	78.5
Latent heat of evaporation (kJ/kg)	420	845

In this paper, a simple stoichiometric AFR estimation law using the exhaust oxygen sensor is proposed, analyzed and discussed in light of AFR control, which yields the estimated ethanol percentage in the fuel. Characteristics of the algorithm including sensitivity are quantified via simulations.

ETHANOL CONTENT ESTIMATION

Air-to-fuel ratio control around the stoichiometric ratio of a fuel blend is important to meet stringent emission requirements for spark ignition (SI) engines. For a given air charge, the stoichiometric fuel is typically achieved by a combination of feedforward and feedback control on the fuel injection. The feedback controller is based on the measured ratio (λ) of the actual air-to-fuel ratio (AFR) to the stoichiometric ratio (AFR_s) through an exhaust gas oxygen sensor. The λ ratio is compared to $\lambda^{des} = 1$ and the error is used by a PI to adjust the feedback fuel command. Due to the long delays in the feedback loop, most engine controllers employ a feedforward fuel command which is primarily derived from the estimated cylinder air charge divided by the assumed stoichiometric ratio of the assumed fuel blend. Furthermore, the feedforward is usually designed to eliminate the transient effects of fuel puddle dynamics in port fuel injected (PFI) engines. Since the puddle dynamics is dependent on the ethanol content, estimation of ethanol content may also be used for the transient fuel compensation (TFC). A model of fuel puddle dynamics with alternative fuels is discussed in [8] where a fuel blend is modeled as a certain combination of organic compounds that mimic the distillation behavior of an actual fuel. When the assumed stoichiometric ratio is correct, and there are no errors in the air charge and fuel puddle dynamics estimation, and no drifts or faults in the injector, the feedforward fuel command is then perfect and the feedback fuel compensation should be zero. An estimation algorithm can utilize a nonzero feedback fuel command to adapt and improve the feedforward fuel compensator so that the feedback converges back to its nominal zero value. Ideally, the adaptation will address the core problem in the feedforward path. In the case of an FFV, the adaptation of the assumed stoichiometric ratio or the adaptation for a miscalibrated

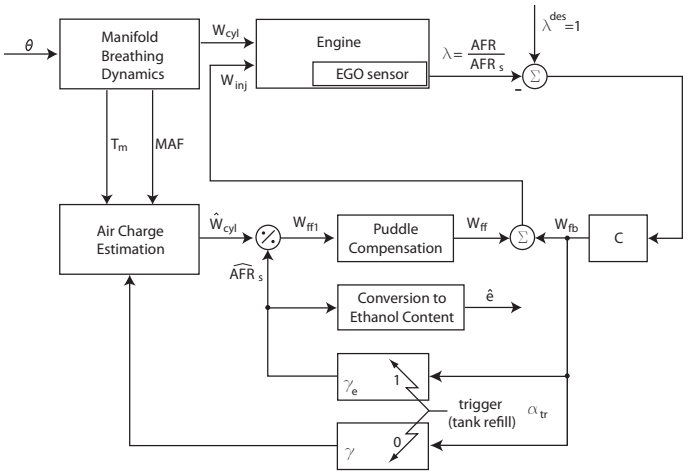

Figure 1. BLOCK DIAGRAM OF AFR CONTROL.

air charge estimation cannot coexist. Namely, the engine management system will have to assume that the error arises from changes in the fuel blend or from component (sensor, actuator) aging.

Fig. 1 shows the block diagram of AFR control with flex fuel. Let e denote the volume fraction of ethanol in gasoline-ethanol blend. And let e_m denote the mass fraction of ethanol. Then, e_m is expressed as:

$$\begin{aligned} e_m &= \frac{e\rho_{eth}}{e\rho_{eth}+(1-e)\rho_{gsl}} \\ &= \frac{e}{e+(1-e)\rho_{gsl}/\rho_{eth}} \\ &= \frac{e}{e+(1-e)/1.056}, \end{aligned} \tag{1}$$

where ρ_{eth} and ρ_{gsl} denote the density of ethanol and the density of gasoline respectively. Now, the stoichiometric air fuel ratio for flex fuel is expressed as:

$$AFR_s = 9\times e_m + 14.6\times(1-e_m). \tag{2}$$

Hence, if we want to calculate the volume fraction of ethanol, e, from an estimated stoichiometric AFR, $\widehat{AFR}_s$, the following equations are utilized:

$$\widehat{e}_m = \frac{14.6-\widehat{AFR}_s}{5.6}, \tag{3}$$

$$\widehat{e} = \frac{\widehat{e}_m}{1.056-0.056\times\widehat{e}_m}. \tag{4}$$

A simple adaptation law of ethanol content estimation can be expressed by the following update law of the estimated stoichiometric AFR, $\widehat{AFR}_s$, using the feedback fuel correction signal, W_{fb}. The adaptation law is triggered after a tank refill event

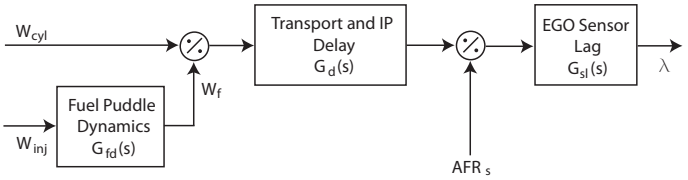

Figure 2. PATH FROM INJECTOR COMMAND TO EGO SENSOR OUTPUT.

is detected ($\alpha_{tr}=1$), otherwise ($\alpha_{tr}=0$) another adaptation loop is typically activated that corrects the engine maps, such as volumetric efficiency used for the air charge estimation, or drifts in sensors and actuators:

$$\dot{\widehat{AFR}}_s = \gamma_e(0-W_{fb})\alpha_{tr}. \tag{5}$$

Then, the feedforward fuel command is determined:

$$W_{ff1} = \widehat{W}_{cyl}/\widehat{AFR}_s, \tag{6}$$

where $\widehat{W}_{cyl}$ is the estimated air charge.

CLOSED-LOOP DYNAMICS

Let us consider the linearized dynamics of the system with the simple AFR estimation law about a fixed stoichiometry and a fixed cylinder air flow associated with a specific load (manifold pressure) and engine speed. Fig. 2 shows the process considered once the fuel command is issued to the injectors all the way until λ is measured by the EGO sensor (engine block of Fig. 1). We assume that the fuel puddle dynamic behavior is expressed as a LTI transfer function in the neighborhood of the chosen equilibrium point given by:

$$G_{fd}(s) = \frac{(1-X)\tau s+1}{\tau s+1}, \tag{7}$$

where X and τ are Aquino parameters which denote the wall-impacting portion of the injected fuel and the vaporization time constant of the fuel puddle, respectively. Let the Padé approximation of the transport and induction-to-power (IP) delay from the cylinder input AFR to the exhaust AFR be:

$$G_d(s) = \frac{1-\frac{\tau_d}{2}s}{1+\frac{\tau_d}{2}s}, \tag{8}$$

where τ_d is the delay time. And let us express the λ sensor lag as:

$$G_{sl}(s) = \frac{1}{1+\tau_s s}, \tag{9}$$

where τ_s is the time constant of the sensor lag. Then, the λ output is expressed as:

$$\lambda = G_{sl}(s)\left\{\left(G_d(s)\left(\frac{W_{cyl}}{W_f}\right)\right)/AFR_s\right\}, \tag{10}$$

where W_{cyl} denotes the air flow rate into the cylinder, W_f the fuel flow rate into the cylinder and AFR_s the stoichiometric air fuel ratio. W_f is the fuel that effectively enters the cylinder related with the fuel injection rate, W_{inj}, by the fuel dynamics such that

$$W_f = G_{fd}(s)W_{inj}. \tag{11}$$

Let us define $G(s)$ as:

$$G(s) \triangleq G_{fd}(s)G_d(s)G_{sl}(s). \tag{12}$$

The control law without the feedforward compensation of the fuel dynamics can be summarized as:

$$W_{inj} = W_{ff} + W_{fb}, \tag{13}$$
$$W_{ff} = \widehat{W}_{cyl}/\widehat{AFR}_s, \tag{14}$$
$$W_{fb} = -C_{fb}(s)(1-\lambda), \tag{15}$$
$$\widehat{\dot{AFR}}_s = -\gamma_e W_{fb}, \tag{16}$$

where the feedback controller, $C_{fb}(s)$, is assumed to be a PI controller:

$$C_{fb}(s) = k_{PI}\frac{\tau_{PI}s+1}{s}. \tag{17}$$

Note that here the air flow rate into the cylinder is assumed to be exactly estimated, $\widehat{W}_{cyl} = W_{cyl}$, for the PI gain tuning analysis. The closed-loop system is expressed by the set of equations of (10), (11) and (13)-(16). We use the superscript ^{0} to express a nominal value at equilibrium and use δ to express the deviation from the equilibrium. Equation (10) is then linearized into:

$$\begin{aligned}\delta\lambda &= G_{sl}(s)\left\{G_d(s)\left(\frac{1}{W_{cyl}^0}\delta W_{cyl} - \frac{1}{W_f^0}\delta W_f\right) - \frac{1}{AFR_s^0}\delta AFR_s\right\} \\ &= \frac{1}{W_{cyl}^0}G_d(s)G_{sl}(s)\delta W_{cyl} - \frac{1}{W_f^0}G(s)\delta W_{inj} \\ &\quad -\frac{1}{AFR_s^0}G_{sl}(s)\delta AFR_s.\end{aligned} \tag{18}$$

From Eq. (13)-(16), we obtain:

$$\delta W_{inj} = \delta W_{ff} + \delta W_{fb}, \tag{19}$$
$$\delta W_{ff} = \frac{1}{AFR_s^0}\delta W_{cyl} - \frac{W_f^0}{AFR_s^0}\delta\widehat{AFR}_s, \tag{20}$$
$$\delta W_{fb} = C_{fb}(s)\delta\lambda, \tag{21}$$
$$\delta\widehat{AFR}_s = -\frac{\gamma_e}{s}\delta W_{fb}. \tag{22}$$

Using Eq. (21) and Eq. (22), δW_{ff} in Eq. (20) is expressed as:

$$\delta W_{ff} = \frac{1}{AFR_s^0}\delta W_{cyl} + \gamma_e\frac{W_f^0}{AFR_s^0}\cdot\frac{1}{s}\cdot C_{fb}(s)\delta\lambda. \tag{23}$$

The total injection signal is then expressed as:

$$\delta W_{inj} = \frac{1}{AFR_s^0}\delta W_{cyl} + \left(\gamma_e\frac{W_f^0}{AFR_s^0}\cdot\frac{1}{s}+1\right)C_{fb}(s)\delta\lambda. \tag{24}$$

Equation (24) is substituted into the equation (18) to obtain the closed loop transfer functions.

$$R(s)\delta\lambda = \frac{1}{W_{cyl}^0}\left(G_d(s)G_{sl}(s) - G(s)\right)\delta W_{cyl} - \frac{1}{AFR_s^0}G_{sl}(s)\delta AFR_s,$$

where $R(s)$ is defined as:

$$R(s) \triangleq 1 + \frac{1}{W_f^0}\left(\gamma_e\frac{W_f^0}{AFR_s^0}\cdot\frac{1}{s}+1\right)G(s)C_{fb}(s). \tag{25}$$

The linearized disturbance input-output relation is expressed as the following closed-loop system:

$$\delta\lambda = T_1(s)\delta W_{cyl} + T_2(s)\delta AFR_s, \tag{26}$$

where the closed-loop transfer functions, $T_1(s)$ and $T_2(s)$, are defined as:

$$T_1(s) \triangleq \frac{1}{W_{cyl}^0}\cdot\frac{G_d(s)G_{sl}(s) - G(s)}{R(s)}, \tag{27}$$
$$T_2(s) \triangleq -\frac{1}{AFR_s^0}\frac{G_{sl}(s)}{R(s)}. \tag{28}$$

The closed-loop transfer functions are expressed as:

$$T_1(s) = \frac{1}{W_{cyl}^0}\cdot\frac{X\tau s^3(1-\frac{\tau_d}{2}s)}{D(s)}, \tag{29}$$
$$T_2(s) = -\frac{1}{AFR_s^0}\cdot\frac{s^2(\tau s+1)(1+\frac{\tau_d}{2}s)}{D(s)}, \tag{30}$$

where $D(s) \triangleq s^2(1+\frac{\tau_d}{2}s)(1+\tau_s s)(\tau s+1)R(s)$.

$$D(s) = s^2\left(1+\frac{\tau_d}{2}s\right)(1+\tau_s s)(\tau s+1) + k_{PI}\cdot \left(\frac{\gamma_e}{AFR_s^0}+\frac{1}{W_f^0}\cdot s\right)((1-X)\tau s+1)\left(1-\frac{\tau_d}{2}s\right)(\tau_{PI}s+1). \quad (31)$$

Since we want the estimated stoichiometric AFR, $\widehat{AFR}_s$, to track the real stoichiometric AFR, AFR_s, we consider the closed-loop linearized error dynamics also. First, we define the estimation error variable, $\varepsilon_{AFR_s} \triangleq AFR_s - \widehat{AFR}_s$. We then can find the linearized disturbance input-estimation error relation:

$$\begin{aligned}
\delta\varepsilon_{AFR_s} &= \delta AFR_s - \delta\widehat{AFR}_s \\
&= \delta AFR_s + \frac{\gamma_e}{s}\delta W_{fb} \\
&= \delta AFR_s + \frac{\gamma_e}{s}C_{fb}(s)\delta\lambda \\
&= \delta AFR_s + \frac{\gamma_e}{s}C_{fb}(s)\left(T_1(s)\delta W_{cyl} + T_2(s)\delta AFR_s\right) \\
&= \frac{\gamma_e}{s}C_{fb}(s)T_1(s)\delta W_{cyl} + \left(1+\frac{\gamma_e}{s}C_{fb}(s)T_2(s)\right)\delta AFR_s \\
&\triangleq T_3(s)\delta W_{cyl} + T_4(s)\delta AFR_s, \qquad (32)
\end{aligned}$$

where the closed-loop transfer functions, $T_3(s)$ and $T_4(s)$, are expressed as:

$$T_3(s) = \frac{1}{W_{cyl}^0}\cdot\frac{\gamma_e k_{PI}X\tau s(\tau_{PI}s+1)(1-\frac{\tau_d}{2}s)}{D(s)}, \qquad (33)$$

$$T_4(s) = 1 - \frac{1}{AFR_s^0}\cdot\frac{\gamma_e k_{PI}(\tau_{PI}s+1)(\tau s+1)(1+\frac{\tau_d}{2}s)}{D(s)}. \qquad (34)$$

In summary, the augmented closed-loop system is expressed as:

$$\begin{bmatrix}\delta\lambda \\ \delta\varepsilon_{AFR_s}\end{bmatrix} = \begin{bmatrix}T_1(s) & T_2(s) \\ T_3(s) & T_4(s)\end{bmatrix}\begin{bmatrix}\delta W_{cyl} \\ \delta AFR_s\end{bmatrix}. \qquad (35)$$

It is easy to check that the DC gains of the closed-loop transfer functions, $T_1(s)$, $T_2(s)$, $T_3(s)$ and $T_4(s)$ are all zero with positive gains, which implies the disturbance rejection characteristic for the output and for the estimation error. Therefore, the λ output asymptotically tracks one, the stoichiometry, and the estimation of stoichiometric AFR asymptotically converges to the real stoichiometric AFR if positive gains can be found that guarantee stability and good performance for all the four transfer functions in Eq. (35).

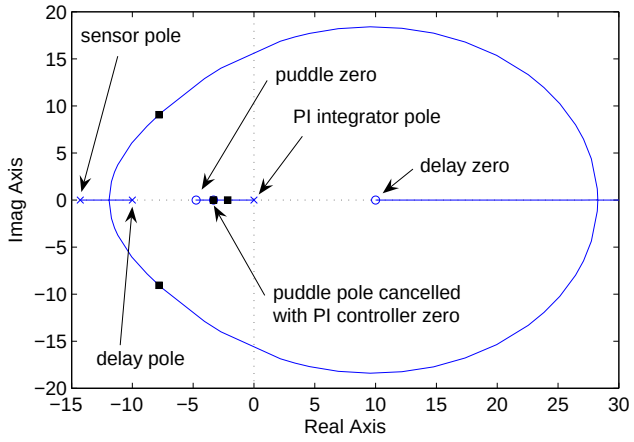

Figure 3. ROOT LOCUS WITH THE VARIATION OF k_{PI}.

CONTROLLER TUNING

PI Gain Tuning of the λ Feedback Controller

For the gain tuning of the feedback PI controller, consider the system of a fixed stoichiometry without the stoichiometric AFR estimation. This is equivalent to setting $\gamma_e = 0$ and $\delta AFR_s = 0$ in the closed-loop dynamics equation (26). The closed-loop dynamic behavior is then expressed as:

$$\delta\lambda = \frac{1}{W_{cyl}^0}\cdot\frac{G_d(s)G_{sl}(s)-G(s)}{1+\frac{1}{W_f^0}G(s)C_{fb}(s)}\delta W_{cyl}. \qquad (36)$$

The variable τ_{PI} in the PI feedback controller can be determined by placing the controller zero to cancel the slowest stable pole of $G(s)$. If the slowest pole is associated with the fuel dynamics, we can set $\tau_{PI} = \tau$. The root locus with variation of k_{PI} can then be utilized to tune the gain, k_{PI}. Fig. 3 shows the root locus of the closed-loop transfer function with the variation of k_{PI} for a fixed τ_{PI}. To obtain the locus in Fig. 3, the engine parameters were chosen as:

$$X = 0.3,\ \tau = 0.3 \text{ sec},\ \tau_d = 0.2 \text{ sec},\ \tau_s = 0.07 \text{ sec}\ .$$

And the PI control gains were tuned to:

$$\tau_{PI} = 0.3,\ k_{PI} = 0.0015\ .$$

Ethanol Estimator Gain Tuning

In order to tune the estimator gain, γ_e, the root locus is applied for the $D(s)$ in Eq.(31) for a set of fixed feedback gains, τ_{PI} and k_{PI}, determined by the method of the previous subsection. Fig. 4 shows the root locus of the original closed-loop transfer functions with the variation of γ_e for a set of fixed feedback gains previously tuned. The estimator gain was chosen as:

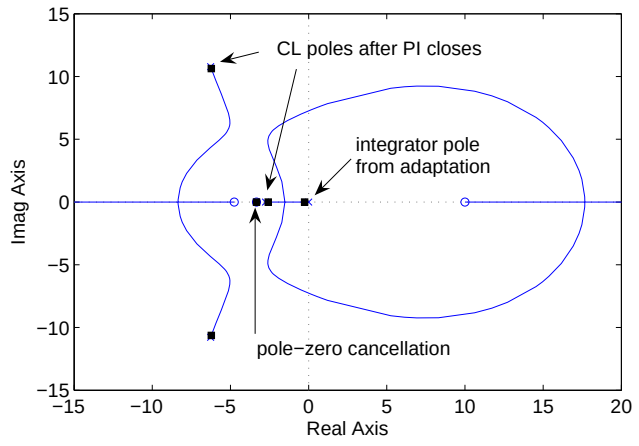

Figure 4. ROOT LOCUS WITH THE VARIATION OF γ_e.

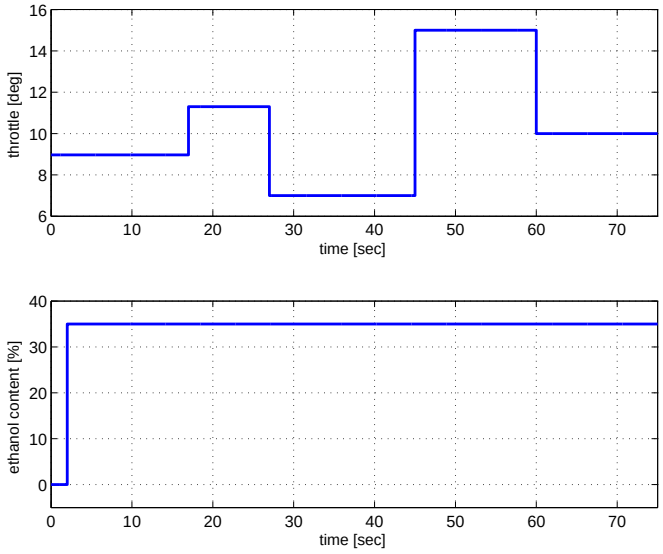

Figure 5. SIMULATION INPUT.

$$\gamma_e = 5000$$

We can also determine the range of γ_e for stability from the locus. The estimator gain where the roots cross the imaginary axis in the locus (Fig. 4) is $\gamma_e = 1.7 \times 10^5$. Note that the chosen estimation gain is very small because a large value for γ_e affects the numerator of both transfer functions, $T_3(s)$ and $T_4(s)$, and hence poor transient response.

SIMULATION RESULTS

Simulations were performed to see the disturbance rejection characteristic under perturbations in the cylinder air flow induced by tip-ins and tip-outs and a perturbation in the stoichiometric AFR emulating a tank refill with unknown ethanol content fuel.

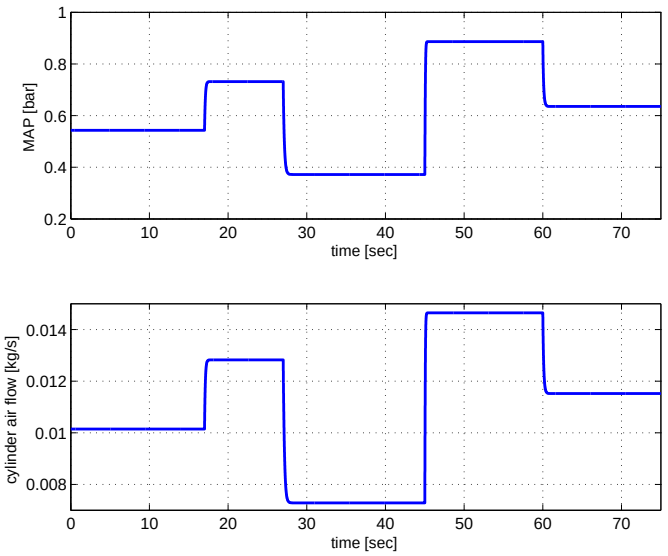

Figure 6. MANIFOLD ABSOLUTE PRESSURE AND AIR FLOW RATE INTO THE CYLINDER INDUCED BY THROTTLE INPUT.

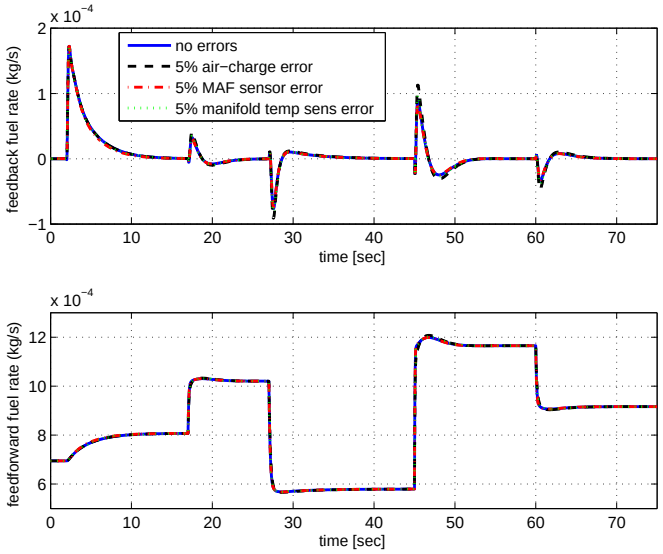

Figure 7. SIMULATED FEEDBACK FUEL SIGNAL AND FEEDFORWARD FUEL SIGNAL.

Errors in air-charge estimation, mass air flow (MAF) sensor and manifold temperature sensor were also introduced with an error factor of 5% at a time to check the sensitivity of the ethanol estimation. The engine model introduced by Crossley and Cook [9] was utilized while maintaining the engine speed at 2000 RPM for throttle-to-cylinder air charge dynamics. The PI control gains and the estimator gain were determined as previously discussed: $\tau_{PI} = 0.3$, $k_{PI} = 0.0015$ and $\gamma_e = 5000$. The roots corresponding to the selected gains are marked as points on the root loci of

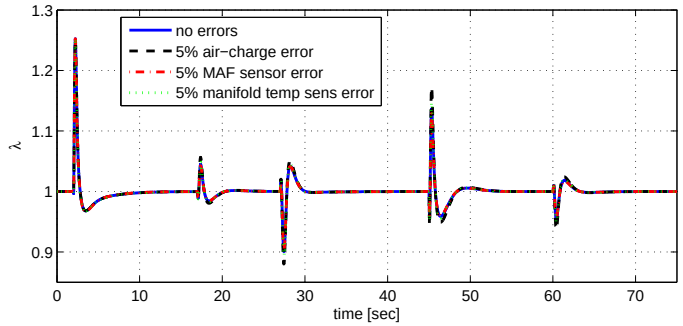

(a) λ output for the whole time span of the simulation

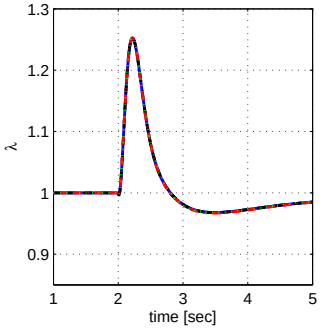

(b) λ output during 1-5 seconds

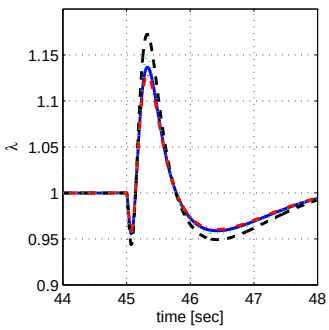

(c) λ output during 44-48 seconds

Figure 8. SIMULATED λ.

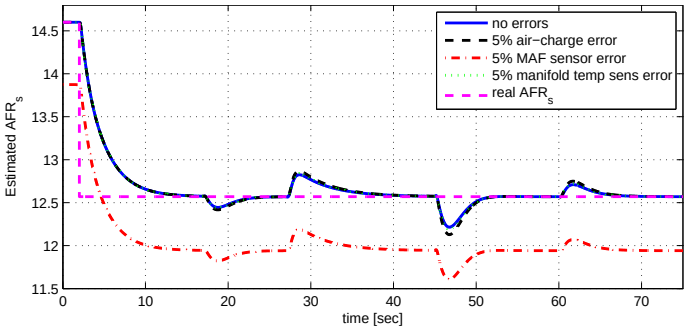

Figure 9. SIMULATED STOICHIOMETRIC AFR ESTIMATION.

Fig. 3 and Fig. 4. Fig. 5 shows the simulation input. Throttle angles were modulated with a sequence of step changes and also a step change of real ethanol content was applied. Initially the fuel used is gasoline and then it is changed to E35. Because of this fuel change, different fuel dynamics parameters were used during the time span of E35 to account for the dynamics dependency on the fuel composition:

$$X_{E35} = 0.361$$
$$\tau_{E35} = 0.4287$$

Fig. 6 shows the change in the manifold absolute pressure and the air flow rate into the cylinder induced by the throttle modulation. Fig. 7-10 show the simulation results. λ and the estimated ethanol content asymptotically track their desired values. The λ error is very sensitive to an air-charge error. It is also moderately sensitive to manifold temperature sensor error; it is insensitive to MAF sensor error. The estimated stoichiometric AFR or the estimated ethanol content converges to the real value except for the case of MAF sensor error where the steady-state ethanol percent estimation shows a 30% sensitivity. Hence, errors in the conventional sensors used in AFR control should be taken into account and ideally corrected through other redundancies. In some sense the "sensorless estimation of ethanol content" is a misnomer and rigorous model-based engineering analysis should be pursued to minimize sensitivities using a combination of many sensors.

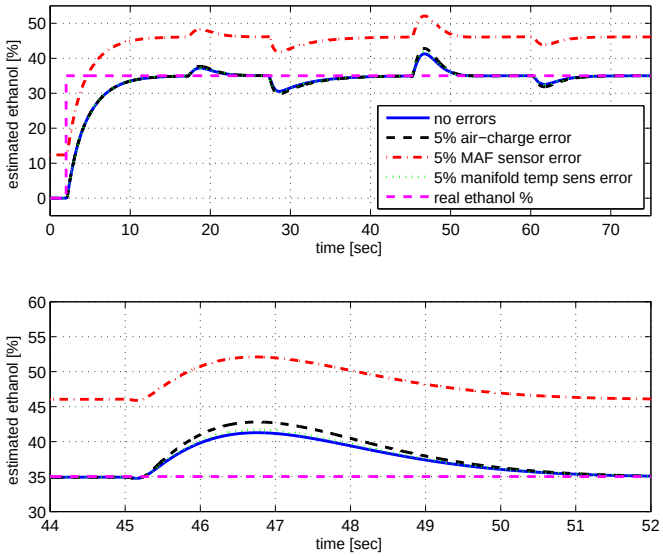

Figure 10. SIMULATED ETHANOL CONTENT ESTIMATION.

STEADY-STATE ERROR ANALYSIS

It is rather straightforward to analytically calculate how various modeling errors or sensor/actuator drifts propagate to cause steady-state errors in the ethanol estimation. Since the simulations in the previous sections indicate a high error sensitivity to MAF sensor drift, an analytical steady-state error calculation is provided below. Let f_e be the MAF sensor error fraction so that the estimated air flow rate into the cylinder in the steady state be expressed as

$$\widehat{W}_{cyl} = (1+f_e)W_{cyl}. \tag{37}$$

The fuel injection or fuel flow rate into the cylinder is expressed as:

$$W_f = \frac{\widehat{W}_{cyl}}{\widehat{AFR}_s}. \tag{38}$$

Due to the λ PI-based feedback loop, λ is regulated at unity, and consequently, the actual steady-state AFR is regulated at the stoichiometric value independently of the fuel.

$$AFR_s = AFR = \frac{W_{cyl}}{W_f} = \frac{W_{cyl}}{\widehat{W}_{cyl}} \cdot \widehat{AFR}_s = \frac{1}{1+f_e}\widehat{AFR}_s. \quad (39)$$

If the stoichiometric air-to-fuel ratio is expressed by the mass fraction of ethanol, the following equation is obtained:

$$\frac{9 \times e_m + 14.6 \times (1-e_m)}{9 \times \hat{e}_m + 14.6 \times (1-\hat{e}_m)} = \frac{1}{1+f_e}, \quad (40)$$

where e_m and $\hat{e}_m$ are the actual mass fraction of ethanol and the estimated mass fraction of ethanol, respectively. The estimated mass fraction of ethanol, $\hat{e}_m$, is then expressed as a function of f_e and e_m:

$$\hat{e}_m = e_m - f_e\left(\frac{14.6}{5.6} - e_m\right). \quad (41)$$

The estimated volume fraction of ethanol, $\hat{e}$ can be then calculated by Eq. (4). Fig. 11 shows the volumetric ethanol content estimation with 5% MAF sensor error.

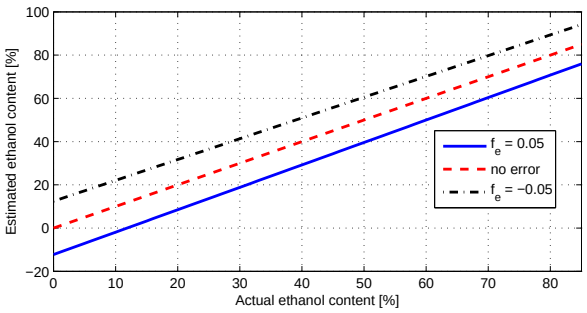

Figure 11. ETHANOL CONTENT ESTIMATION IN THE STEADY STATE WITH 5% MAF SENSOR ERROR

CONCLUSION

In this paper, estimation of the ethanol content in flex-fuel vehicles using a λ-based approach is demonstrated with a model. Tuning and sensitivity are also studied. The linearized closed-loop dynamics are derived to present the disturbance rejection characteristic for λ and the ethanol estimation error. PI gain tuning for the fuel feedback control and the ethanol estimation gain tuning are shown with root loci. Simulations show high sensitivity of the ethanol estimation, thus motivating the need for redundant algorithms with fusion of many sensors. Future work will include minimization of sensitivity, feedforward compensation of fuel puddle dynamics with an invertible puddle dynamics model for flex-fuel and the analysis of switching between the two adaptation loops, i.e., the ethanol content estimation and the correction of engine maps used for the air charge estimation.

REFERENCES

[1] Delgado, R.C.O.B., Araujo, A.S. and Fernandes Jr., V.J., 2007. "Properties of Brazilian gasoline mixed with hydrated ethanol for flex-fuel technology," *Fuel Processing Technology*, 88, pp. 365-368.

[2] Nakata, K., Utsumi, S., Ota, A., Kawatake, K., Kawai, T. and Tsunooka, T., "The Effect of Ethanol Fuel on a Spark Ignition Engine," *SAE paper 2006-01-3380*.

[3] Cowart, J.S., Boruta, W.E., Dalton, J.D., Dona, R.F., Rivard II, F.L., Furby, R.S., Piontkowski, J.A., Seiter, R.E. and Takai, R.M., "Powertrain Development of the 1996 Ford Flexible Fuel Taurus," *SAE paper 952751*.

[4] Stodart, A., Maher, J., Greger, L. and Carlsson, J., "Fuel System Development to Improve Cold Start Performance of a Flexible Fuel Vehicle," *SAE paper 982532*.

[5] Orbital Engine Co., 2002. "A Literature Review Based Assessment on the Impacts of a 20% Ethanol Gasoline Fuel Blend on the Australian Vehicle Fleet," *Report to Environment Australia*, Nov.

[6] Bromberg, L., Cohn, D.R. and Heywood, J.B., 2007. "Optimized Fuel Management System for Direct Injection Ethanol Enhancement of Gasoline Engines," *United States Patent No. US 7,225,787 B2*.

[7] Theunissen, F.M.M., "Percent Ethanol Estimation on Sensorless Multi Fuel Systems; Advantages and Limitations," *SAE paper 2003-01-3562*.

[8] Batteh, J.J. and Curtis, E.W., "Modeling Transient Fuel Effects with Alternative Fuels," *SAE paper 2005-01-1127*.

[9] Crossley, R.R. and Cook, J.A., IEE International Conference 'Control 91,' Conference Publication 332, vol. 2, pp. 921-925, 25-28 March, 1991, Edinburgh, U.K.